Transcriptome changes induced by *RUNX3* in cervical cancer cells *in vitro*

QIAN-QIAN GAO[1], BIN ZHOU[2], XIU-ZHANG YU[3], ZHU ZHANG[3], YAN-YUN WANG[2], YA-PING SONG[2], LIN ZHANG[2], HONG LUO[1] and MING-RONG XI[3]

[1]Department of Ultrasound; [2]Laboratory of Molecular Translational Medicine, West China Institute of Women and Children's Health, Key Laboratory of Obstetric and Gynecological and Pediatric Diseases and Birth Defects of Ministry of Education; [3]Department of Obstetrics and Gynecology, West China Second University Hospital, Sichuan University, Chengdu, Sichuan 610041, P.R. China

Received March 2, 2019; Accepted September 6, 2019

DOI: 10.3892/ol.2019.11128

Abstract. Runt-related transcription factor 3 (*RUNX3*) is a member of Runt domain family that is known to play key roles in various different types of tumor. It was recently demonstrated that *RUNX3* may also be associated with cervical cancer. The aim of the present study was to investigate the potential association between transcriptome changes and *RUNX3* expression in cervical cancer. A *RUNX3* overexpression model was constructed using cervical cancer cell lines by *RUNX3* plasmid transfection. It was demonstrated that the upregulated expression of *RUNX3* inhibited proliferation of cervical cancer cell lines, particularly SiHa cells, and was associated with the expression of the *IL-6*, *PTGS2*, *FOSL1* and *TNF* genes. In addition, it was revealed that the *TNF* and *FoxO* pathways may also be affected by *RUNX3*. Therefore, the expression of the *RUNX3* gene may be involved in the occurrence and progression of cervical cancer.

Introduction

Cervical cancer was reported as the most common gynecological tumor in developing countries in 2012 (1). It was also estimated that 527,600 women were first diagnosed with cervical cancer and 265,700 women succumbed to this disease worldwide in the same year (1). In recent years, cervical cytology screening and vaccination have been used to prevent cervical cancer development due to human papillomavirus (HPV) infection (2). However, thousands of women are still affected by cervical cancer, with detrimental effects on their quality of life (3). Alongside the increased amount of research that makes the molecular mechanism underlying cervical cancer more clear, particularly with the knowledge that HPV and E6 oncoproteins potentially affect the progress of cervical cancer, an increasing number of genes have been demonstrated to be implicated in cervical cancer (4,5). Identifying new molecular targets for the prevention and treatment of cervical cancer would further improve the quality of life of the patients.

Runt-related transcription factor 3 (*RUNX3*), along with *RUNX1* and *RUNX2*, are members of the Runt domain family (6). *RUNX3* is involved in the transforming growth factor β (TGF-β) signaling pathway, which is a key downstream effector affecting the progression of tumors (7). In a number of previous studies on gastric, hepatocellular and breast cancer, *RUNX3* has been revealed to play a significant role in tumor suppression (8-11). Recent research has demonstrated that *RUNX3* may also act as a tumor suppressor gene in cervical cancer (12). *RUNX3* expression may be suppressed by promoter hypermethylation, gene deletions, inactivating mutations and protein mislocalization (8,11,13-16). By contrast, other researchers concluded that *RUNX3* acts as an oncogene in skin, ovarian and head and neck cancer, where its expression level was observed as significantly increased (17-20). In addition, Lotem *et al* (21) hypothesized that this gene plays important roles in immunity and inflammation, and may affect the development of epithelial tumors.

In a previous study, it was observed that the polymorphisms of *RUNX3* may be associated with cervical cancer, and the mRNA expression of *RUNX3* was significantly different between the cervical cancer group and the healthy female subjects (22). However, the specific molecular mechanism through which *RUNX3* regulates cancer-associated signaling pathways and affects tumorigenesis remains elusive. The aim of the present study was to investigate the effect of *RUNX3* on cervical cancer cell lines, and to identify the transcriptome changes in cervical cancer.

Materials and methods

Cell culture. SiHa, HeLa and C33A cells were obtained from the Laboratory of Molecular Translational Medicine,

Correspondence to: Dr Ming-Rong Xi, Department of Obstetrics and Gynecology, West China Second University Hospital, Sichuan University, 20, Section 3, Renmin South Road, Chengdu, Sichuan 610041, P.R. China
E-mail: qmrjzz@126.com

Key words: Runt-related transcription factor 3, cervical cancer, transcriptome, tumor necrosis factor, Forkhead box O

West China Institute of Women and Children's Health, Key Laboratory of Obstetric & Gynecological and Pediatric Diseases and Birth Defects of Ministry of Education, West China Second University Hospital, Sichuan University (Sichuan, China). SiHa is an HPV-16 infected cervical cancer cell line, HeLa is an HPV-18 infected cervical cell line, and C33A is an HPV-negative cervical cancer cell line. The cells were cultured in DMEM high-glucose medium at 37˚C in 5% CO_2, supplemented with 10% fetal bovine serum and penicillin/streptomycin (50 U/ml) (both Thermo Fisher Scientific, Inc.). There was no contamination of SiHa and C33A cells by HeLa cells.

Construction of plasmids, RNA interference and transfection. Homo sapiens *RUNX3* mRNA sequence (23) was used to design and identify the *RUNX3* overexpression model and empty plasmid (plasmid EX-NEG-M98; Guangzhou FulenGen Co., Ltd.), was used as the control; in addition, *RUNX3* short-hairpin RNA (shRNA) was designed and identified (Guangzhou FulenGen Co., Ltd.). The following base pairs of shRNA (shRNA31, shRNA32, shRNA33 and shRNA34) and the non-targeting sequence control shRNA (shRNA001) were used for *RUNX3* gene interference (Table I). After the single clones were obtained, the extracted plasmids were identified and sequenced via digestion, following the instructions of endotoxin-free plasmid extraction kit (Tiangen Biotech Co., Ltd.). Briefly, 8 ml buffer P1 with RNase A was added to the collected bacteria and vortexed. Subsequently, 8 ml buffer P2 was added, and the samples were shaken gently and left to stand at 25˚C for 5 min. This was repeated with buffer P4, after which the samples were centrifuged at 8,228 x g for 10 min at 25˚C. Following which, 0.3 of the volume of isopropanol and 2.5 ml buffer BL was added, and the samples were transferred to CP6 columns and centrifuged at 8,228 x g for 2 min at 25˚C, twice. A total of 10 ml buffer PW with absolute ethanol was added and the samples were centrifuged at 8,228 g for 2 min at 25˚C, twice. Subsequently, cervical cancer cells were transfected with *RUNX3* overexpression plasmid or shRNA (0.5 μg plasmid) by X-tremeGene HP DNA Transfection Reagent (Roche Diagnostics). In the present study, cells with *RUNX3* overexpression were referred to as 'ORF' *RUNX3* cells, the empty plasmid was the control of ORF *RUNX3* cells as 'NEG' control cells, and those with *RUNX3* shRNA as 'shRNA' *RUNX3* cells. In addition, the control groups were treated only with transfection reagent in SiHa, HeLa and C33A cells, respectively which were referred to as 'Control', and without any intervention as 'cell line name' (baseline controls). At 24, 48 and 72 h after transfection, the cells were harvested and prepared for subsequent experiments.

RNA isolation and reverse transcription-quantitative PCR (RT-qPCR) analysis. Total RNA was extracted from cervical cancer cells and purified using TRIzol® reagent according to the manufacturer's protocol (Thermo Fisher Scientific, Inc.). RT-PCR was performed using a One-Step RT-PCR kit (Bioneer), according to the manufacturer's protocol. RT-qPCR was performed using the SYBR Green PCR Master Mix (Roche Diagnostics). The samples of all genes were amplified in a thermocycler as follows: 95˚C for 10 min (1 cycle), 95˚C for 15 sec and 60˚C for 1 min (48 cycles). The primer sequences are presented in Table II. Data were normalized against β-actin expression with the comparative quantification cycle method. Triplicate Cq values were averaged and the relative expression levels were determined as $2^{-\Delta\Delta Cq}$ (24).

WST-1 measurement and flow cytometry. WST-1 measurement was used to detect cell viability using a WST-1 cell proliferation and cytotoxicity assay kit (Boster Biological Technology Co., Ltd.) according to the manufacturer's protocol. Briefly, the cervical cancer cells were seeded at a density of 10^4 cells/ml into 96-well plates and incubated overnight at 37˚C. Subsequently, the plasmids were transfected into cancer cells for 24/48/72 h 3 times, as aforementioned. WST-1 (10 μl) was added, followed by incubation for a further 2 h at 37˚C. In order to exclude the effect of the WST-1 reagent, the same concentrations of transfection reagent were added to the cells directly when the WST-1 measurement was performed. The absorbance of cells was monitored at 450 nm.

Apoptosis was also analyzed via flow cytometry. First, the transfected tumor cells in each group were lysed with trypsin without EDTA (HyClone; GE Healthcare Life Sciences), and the cells were stained using the FITC Annexin V Apoptosis Detection kit with propidium iodide (PI; both BestBio, http://bestbio.bioon.com.cn/). Finally, for the cell cycle analysis, cells in each group were stained with PI and then analyzed by flow cytometry (Guava® easyCyte™), using nCyte v2.7 software (both EMD Millipore; Merck KGaA).

Transcriptome sequencing. A total of 3 μg RNA from each sample was used, which was prepared for input material of the RNA samples. Sequencing libraries were generated, using the NEBNext® Ultra™ RNA Library Prep kit for Illumina® (New England Biolabs) according to the manufacturer's protocol. The index codes were added to assign sequences to each sample. Briefly, mRNA was purified from total RNA using poly-T oligo-attached magnetic beads NEBNext® Ultra™ Directional RNA Library Prep kit for Illumina® (New England Biolabs, Inc.) according to the manufacturer's protocol. Fragmentation was then performed using divalent cations at increasing temperatures of 25˚C for 10 min, 42˚C for 15 min, and 70˚C for 15 min after which the samples were held at 4˚C, in NEBNext First-Strand Synthesis Reaction Buffer (5X) (New England Biolabs, Inc.). Finally, the PCR products were purified (AMPure XP system), and the library quality was assessed on the Agilent Bioanalyzer 2100 system. According to the manufacturer's instructions, clustering of the index-coded samples was performed on a cBot Cluster Generation System, which used a TruSeq PE Cluster kit v3-cBot-HS (Illumina, Inc.). The library preparations were then sequenced on an Illumina Hiseq 2000/2500 platform, and 100/50 bp single-end reads were generated. Gene Ontology (GO; http://geneontology.org) enrichment analysis of differentially expressed genes was implemented by the GOseq R package (clusterProfiler v3.4.4; http://bioconductor.org/), in which gene length bias was corrected. GO terms with corrected $P<0.05$ were considered significantly enriched by differentially expressed genes. The Kyoto Encyclopedia of Genes and Genomes (KEGG; http://www.genome.jp/kegg) is a database resource for understanding high-level functions and utilities of the biological system, such as the cell, the organism and the ecosystem, from

Table I. shRNAs used in the present study.

Clone name	Symbol	Chromosome location	Length	5'-3'
HSH021393-31-LVRH1GP(OS503663)	*RUNX3*	815	21	GGCAATGACGAGAACTACTCC
HSH021393-32-LVRH1GP(OS545091)	*RUNX3*	159	21	GGAATCCAAATTCTTGGGTAC
HSH021393-33-LVRH1GP(OS503664)	*RUNX3*	2895	21	GGTCTCTTACAGGTATAGTTC
HSH021393-34-LVRH1GP(OS545092)	*RUNX3*	3858	21	GGGATAGTAAATAAATTGCTC
CSHCTR001-1-LVRH1GP(OSNEG20)			19	GCTTCGCGCCGTAGTCTTA

shRNA, short hairpin RNA; *RUNX3*, runt-related transcription factor 3.

Table II. Primer sequences used in the present study.

Gene	Gene ID	Forward (5'-3')	Reverse (5'-3')	Product size, bp
TNC	NM_002160.3	TCGCTACAAGCTGAAGGTGG	GTTAACGCCCTGACTGTGGT	214
PTGS2	NM_000963.3	CAAATTGCTGGCAGGGTTGC	AGGGCTTCAGCATAAAGCGT	139
ICAM1	NM_000201.2	ATGGCAACGACTCCTTCTCG	GCCGGAAAGCTGTAGATGGT	142
TNF SF10	NM_001190942.1	TGCGTGCTGATCGTGATCTT	TCTTGGAGTCTTTCTAACGAGC	234
IL6	NM_000600.3	TTCAATGAGGAGACTTGCCTGG	CTGGCATTTGTGGTTGGGTC	206
IL7R	NM_002185.3	TGAAATATGTGGGGCCCTCG	GTCATTGGCTCCTTCCCGAT	223
FOSL1	NM_005438.4	AGCCCAGCAGAAGTTCCAC	CCTCTTCCTCCGGGCTGAT	227
IL32	NM_001308078	AGACAGTGGCGGCTTATTATGAGG	GCCTCGGCACCGTAATCC	86
TGF-β	NM_000660.4	TATCGACATGGAGCTGGTGAAG	CAGCTTGGACAGGATCTGGC	67
β-actin	NM_001101.3	TGACGTGGACATCCGCAAAG	CTGGAAGGTGGACAGCGAGG	205

molecular-level information, particularly from large-scale molecular datasets generated by genome sequencing and other high-throughput experimental technologies. The present study used clusterProfiler v3.4.4 software (http://bioconductor.org/) in order to test the statistical enrichment of differentially expressed genes in the KEGG pathways. Through this analysis, different genes were identified as potential regulators of cervical cancer, which may be downstream or upstream of *RUNX3*.

Statistical analysis. GraphPad Prism software (version 5.01; GraphPad Software, Inc.) was used for the data analysis and to assess the normal distribution and equal variance of all data. The baseline characteristics of the participants were assessed by Student's t-test and single-factor Pearson's χ^2 test. Only the difference between two groups were evaluated by Student's t test. Differences among multiple groups were evaluated by the one-way ANOVA, followed by Bonferroni's multiple comparisons test. The *RUNX3* mRNA expression levels were compared between transfected cells, or between groups of cervical cancer cells and controls using Bonferroni's multiple comparisons test. P<0.05 was considered to indicate a statistically significant difference. According to transcriptome sequencing, differential expression analysis of two groups was performed using the DESequencing (DESeq) R package (v1.10.1; https://www.bioconductor.org/). DESeq provides statistical analysis for determining differential expression in digital gene expression data using a model based on the negative binomial distribution. The resulting P-values were adjusted using the Benjamini and Hochberg's approach for controlling the false discovery rate. Genes with an adjusted P-value (q value) found by DESeq were classified as differentially expressed. q<0.05 was considered to indicate a statistically significant difference.

Results

Expression of RUNX3 in cervical cancer lines. The efficiency of exogenous *RUNX3* expression and *RUNX3* shRNA in cervical cancer cells was verified via RT-qPCR analysis. The mRNA levels of *RUNX3* were markedly higher in ORF *RUNX3* cells compared with the NEG control group of the three cervical cancer cell lines (P<0.001; Fig. 1), which were also extremely significantly higher than the 'Control' and 'cell name' groups (P<0.001; Fig. 1). It also demonstrated the low expression levels of *RUNX3* in all the control groups, with or without intervention. In addition, the shRNA *RUNX3* and control groups (shRNA001) were significantly different in the three cell lines, particularly in SiHa cells (P<0.001 and P<0.05, respectively; Fig. 2). As the *RUNX3* gene was successfully suppressed by shRNA34 in SiHa, HeLa and C33A cells, particularly the SiHa cell line at 24 (P<0.001) and 48 h (P<0.05), shRNA34 was selected as the interference plasmid for subsequent experiments (Fig. 2).

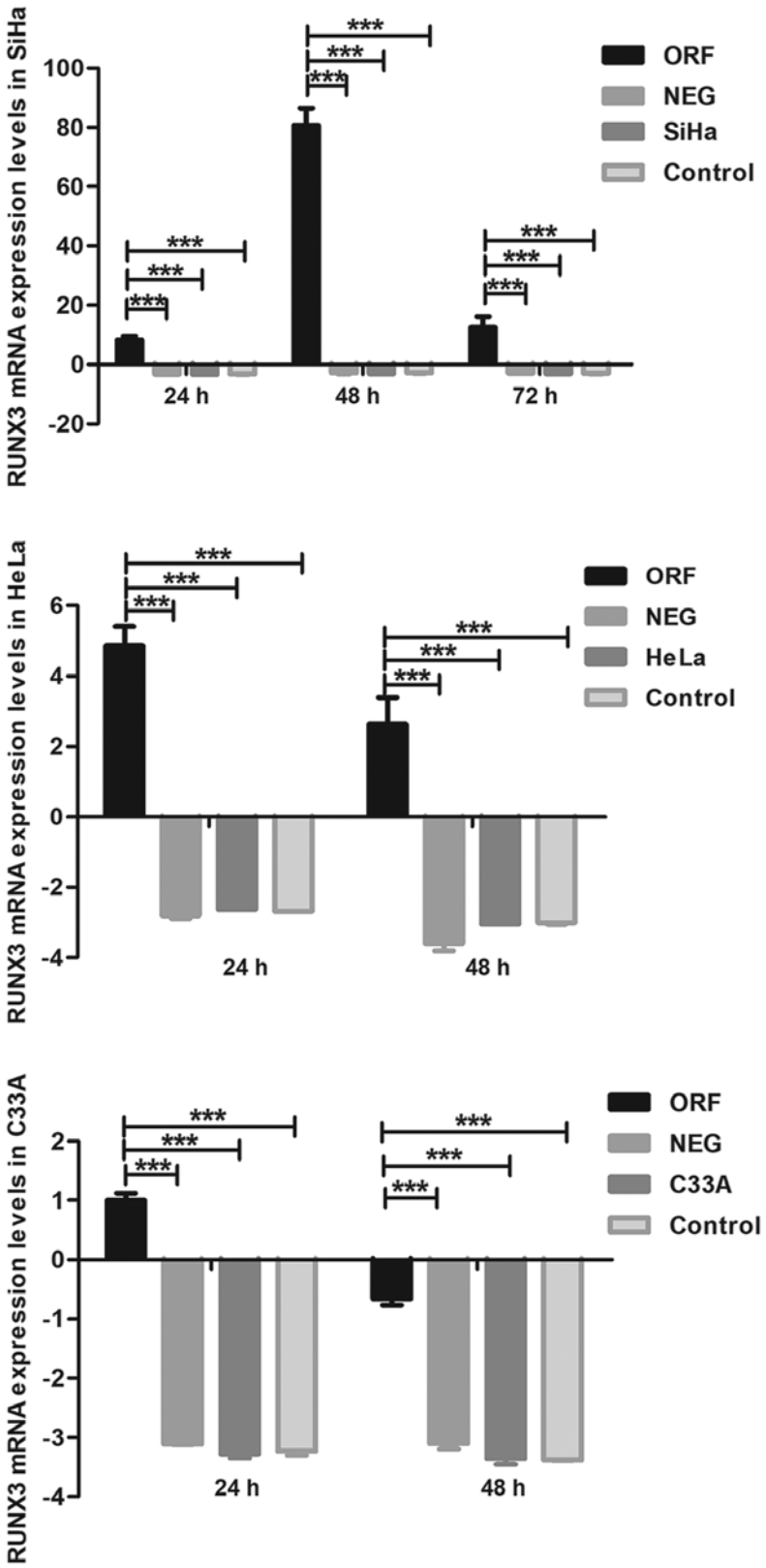

Figure 1. *RUNX3* mRNA expression levels were significantly different between the ORF *RUNX3* cells and NEG control groups in SiHa, HeLa and C33A cell lines. The name of 'SiHa', 'HeLa' and 'C33A' groups were not altered, which were set as baseline controls. ***P<0.001. *RUNX3*, Runt-related transcription factor 3; ORF, *RUNX3* overexpression cells; NEG, empty plasmid-transfected cells.

Role of RUNX3 in proliferation and apoptosis of cervical cancer cells. The WST-1 results suggested that there were significant differences among ORF and NEG plasmid transfection groups and shRNA34 and shRNA001 groups in the SiHa cell line (P<0.05; Fig. 3A), However, the shRNA34 and shRNA001, and ORF and NEG groups exhibited less prominent differences in HeLa and C33A cell lines, respectively, although the results were still significant; (Fig. 3B and C).

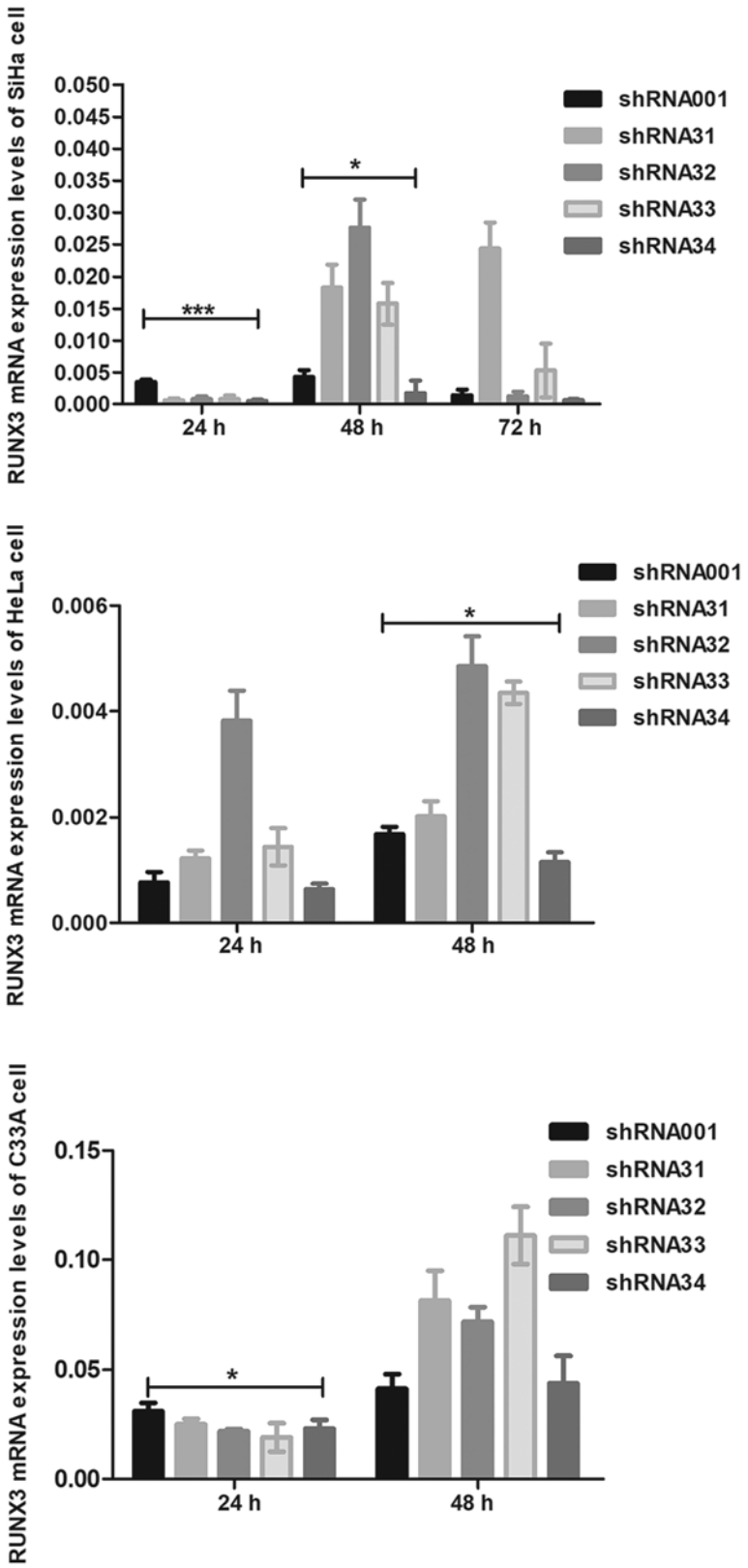

Figure 2. *RUNX3* mRNA expression levels in shRNA *RUNX3* and control groups (shRNA001) differed significantly in SiHa, HeLa and C33A cell lines, particularly between the shRNA34 and shRNA001 groups in SiHa cell. *P<0.05 and ***P<0.001 vs. shRNA001. *RUNX3*, Runt-related transcription factor 3; shRNA, short hairpain RNA.

There was no significant difference between the groups of cervical cancer cells with WST-1 or without WST-1 (Fig. 3). In addition, the results revealed that there were significant differences at different transfection times; the ORF and NEG groups were significantly different at 24, 48, 72 and 96 h in the SiHa cell line, the shRNA34 and shRNA001 groups were significantly different at 72 and 96 h in the HeLa cell line and the ORF and NEG groups were significantly different at 24,

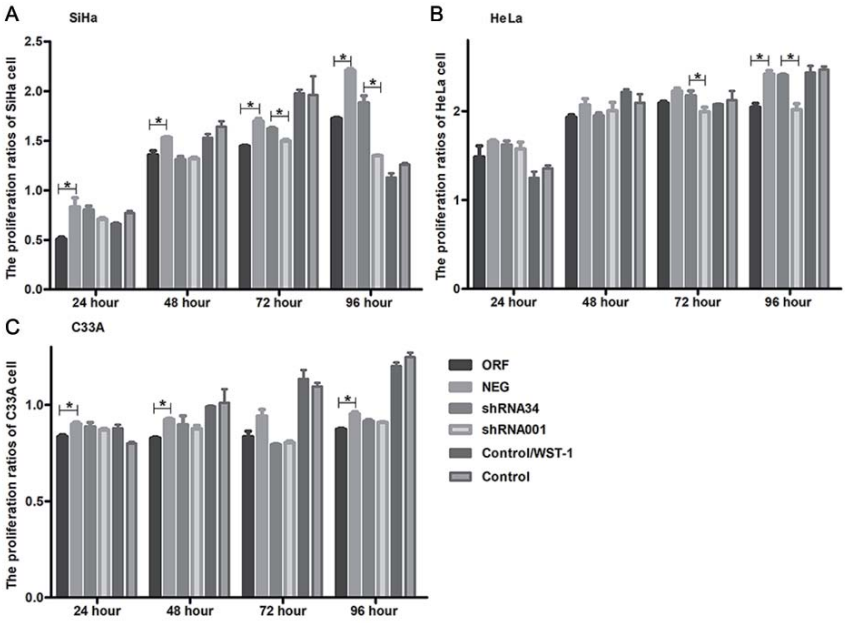

Figure 3. Expression of *RUNX3* affected the proliferation of different cervical cancer cells. (A) The proliferation rate of *RUNX3*-expressing SiHa cells was different at 24, 48, 72 and 96 h. (B) The proliferation rate of *RUNX3*-expressing HeLa cells was different at 72 and 96 h. (C) The proliferation rate of *RUNX3*-expressing C33A cells was different at 24, 48 and 96 h. *P<0.05. *RUNX3*, Runt-related transcription factor 3.

48 and 96 h in the C33A cell line (P<0.05). The results also demonstrated that the effects on different cervical cancer cells varied and indicated that *RUNX3* may inhibit the proliferation of cervical cancer cells.

PI/Annexin V flow cytometry analysis was performed in the present study in order to detect the apoptosis rates in *RUNX3*-transfected cell lines. The apoptosis rates of different cervical cancer cell groups were significantly different, especially in SiHa cells (Fig. 4). The apoptosis rate of the ORF group was significantly higher compared with that in the control group in SiHa cell at 24, 48 and 72 h (P<0.001), indicating an apoptosis-promoting role of *RUNX3* in cervical cancer. Furthermore the apoptosis rate of the shRNA34 group was significantly higher compared with that in the control group at 24, 48 and 72 h, which were inconsistent as expected (P<0.001, Fig. 4). In addition, the apoptosis ratios of HeLa and C33A cells were not significantly higher in the ORF group compared with that in the control group at 24 and 48 h, which were not consistent with those of the SiHa cells in ORF and control group, but in the 48 and 72 h time periods, shRNA34 group was significantly higher compared with that in the control group, in both the HeLa and C33A cells, which is consistent with the SiHa cells (P<0.05; Fig. 4). Finally the apoptosis ratios of ORF group were significantly lower compared with that in the shRNA34 group at 48 h in SiHa, HeLa and C33A cell lines (P<0.05; Fig. 4), and at 72 h in SiHa and HeLa cell lines (P<0.05; Fig. 4). The results may suggest the low expression of *RUNX3* in cervical cancer is complexity to interfere and further research should be preceded.

Effects of RUNX3 on cervical cancer cells by transcriptome sequencing. The molecular mechanisms through which *RUNX3* may affect cervical cancer were investigated in SiHa cells *in vitro*. Relative transcript levels were tested by transcriptome sequencing in order to determine the difference in transcripts mediated by *RUNX3* in SiHa cells. The present study identified 31 genes that were differentially expressed in *RUNX3*-overexpressing SiHa cells. A total of 9 genes showed differences in the three groups simultaneously, including *IL-6*, *PTGS2*, *FOSL1*, *TNC, ICAM1, IL-7R, IL-32, TGF-β* and *TNFSF10* (Figs. 5 and 6), which may be potential regulators of cervical cancer combined with *RUNX3*. The mRNA expressions of the 9 genes confirmed the results of the transcriptome sequencing (Fig. 7), although further research is required to clarify the connection between *RUNX3* and these genes. However, in the shRNA34 groups, except with the *TNC* and *IL-6* gene, the expression levels of these genes were not changed, which may be due to the low expression of *RUNX3* mRNA in cervical cancer and limited interference of shRNA34. Additional research is required in order to develop an improved understanding. Furthermore, following verification of the mRNA expression levels, there was no significant difference between the control groups. In addition, the GO enrichment analysis of biological processes revealed that certain genes were enriched, such as those involved in the regulation of carboxypeptidase, exopeptidase and hydrolase activity. Furthermore, the GO enrichment analyses of the KEGG pathways concluded that these genes were enriched in signaling pathways such as the tumor necrosis factor (*TNF*) pathway, Forkhead box O (*FoxO)* pathway, African trypanosomiasis and malaria (Fig. 8). Transcription factors and proto-oncogenes, such as *HMGA1* and *FOSL1*, *IL7R* and *MALAT1*, were demonstrated as likely to be associated with *RUNX3* in cervical cancer (Fig. 6) and may be associated with microfollicular thyroid adenoma, various benign mesenchymal tumors and renal cell carcinoma (25,26). Finally, the transcriptome sequencing analysis results indicated that two long non-coding RNAs, *RP11-54O7.3* and *MALAT1*, were significantly different between groups, suggesting that *RUNX3* may affect their expression level (Fig. 6). These findings indi-

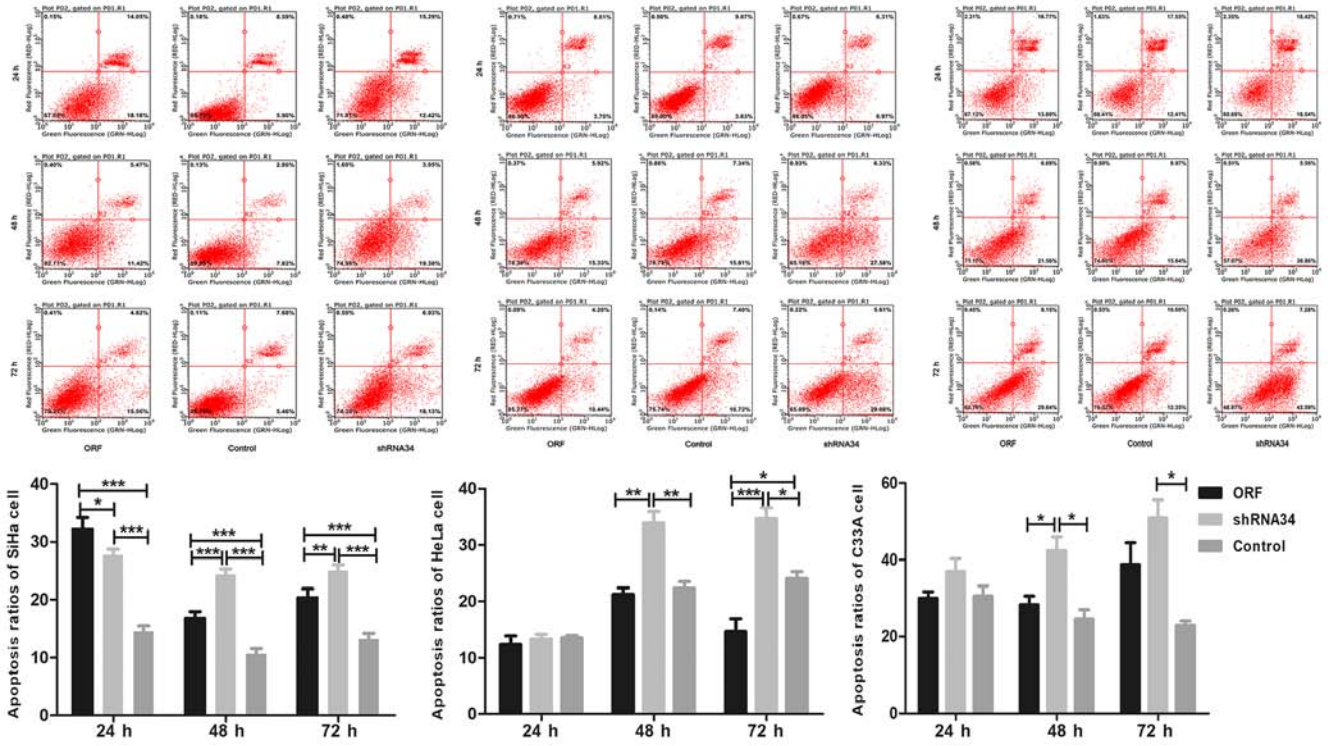

Figure 4. Expression of *RUNX3* affected the apoptosis of different cervical cancer cells. The apoptosis ratios of SiHa cells were significantly different between each group However, *RUNX3* did not affect the apoptosis ratios of HeLa and C33A significantly. *P<0.05, **P<0.01 and ***P<0.001. *RUNX3*, Runt-related transcription factor 3; ORF, *RUNX3* overexpression cells; shRNA, short hairpin RNA.

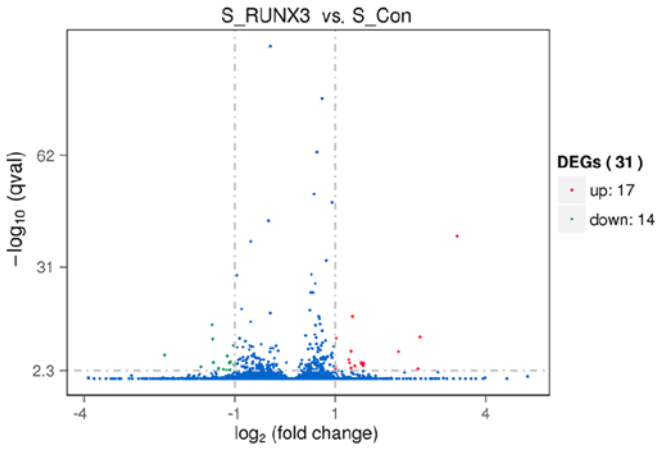

Figure 5. A total of 31 genes were identified as differentially expressed in *RUNX3*-overexpressing SiHa cells with transcriptome sequencing analysis. S_*RUNX3*, *RUNX3*-overexpressing SiHa cells; S_Con, Untransfected SiHa cells. *RUNX3*, Runt-related transcription factor 3; DEGs, differentially expressed genes.

cate that the expression of *RUNX3* may affect the expression of other genes, which may also be associated with cervical cancer *in vitro*.

Discussion

Cervical cancer has been confirmed to be associated with HPV infection; furthermore 0.7% of women initially found to be infected with high-risk HPV will develop invasive carcinomas within 3 years (2,3). In recent years, immunological mechanisms and genetic factors have been demonstrated to play critical roles in cervical cancer (4,27-30). A previous study demonstrated that *RUNX3* is likely a potential gene involved in cervical cancer susceptibility, and was associated with the type of HPV infection and cervical intraepithelial neoplasia progression (22). In the present study, three types of cervical cancer cell lines were selected: SiHa, HeLa and C33A, infected by HPV-16, HPV-18 or not infected, respectively. It was recently reported that *RUNX3* may play a key role in the development and progression of cervical cancer (12). It was also observed in the present study that *RUNX3* may inhibit cervical cancer cell proliferation, particularly in the SiHa cell lines, indicating its potential function as a tumor suppressor; inconsistencies in these results may be due to the different cell lines. In addition, the expression levels of *RUNX3* were lower in the three cell lines, which were almost the same level in the control groups with or without any intervention. The molecular mechanisms and signaling pathways underlying the role of *RUNX3* in cervical cancer remain elusive. The aim of the present study was to elucidate the potential effects of *RUNX3* on cervical cancer by transcriptome sequencing, which may help improve the current therapy options and prognosis of patients with cervical cancer.

It was previously demonstrated that the tumorigenicity of human gastric cancer cell lines was significantly associated with the level of *RUNX3* in nude mice, which suggested that suppression of *RUNX3* function was directly associated with the occurrence and progression of human gastric cancer (9). In a previous study on ovarian cancer, the researchers observed that the overexpression of *RUNX3* in A2780s cells rendered them more resistant to carboplatin, whereas the sensitivity of

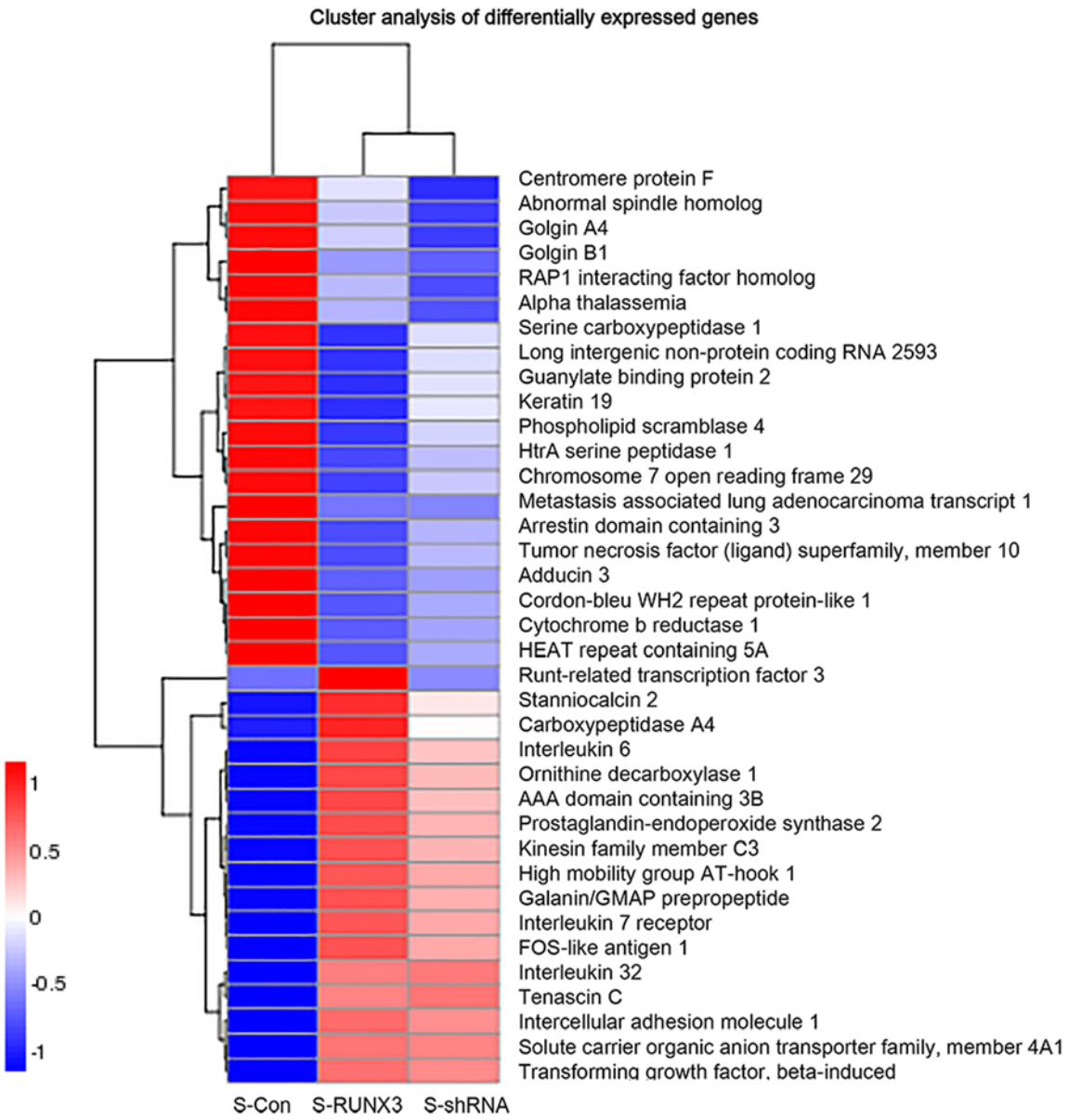

Figure 6. Cluster analysis of differentially expressed genes. The color scale represents re-processed log10 (FPKM+1), with the expression of each gene displayed by colors ranging from red to blue, indicating high to low expression, respectively. FPKM, fragments per kilobase million; *RUNX3*, Runt-related transcription factor 3; shRNA, short hairpin RNA.

A2780cp cells to carboplatin increased significantly following inhibition of *RUNX3* (31). In the present study, the upregulated expression of *RUNX3* consistently inhibited the proliferation and promoted the apoptosis of cervical cancer cells, particularly in the SiHa cell line. The results were similar to those of a recent study on cervical cancer, which reported that upregulated expression of *RUNX3* inhibited the proliferation, migration and invasion of cervical cancer cells (12). According to these results, it may be concluded that *RUNX3* acts as a tumor suppressor gene in cervical cancer (12).

As the mechanisms of action of *RUNX3* have not yet been fully elucidated, the molecular mechanisms and signaling pathways of *RUNX3* have become a focus in cancer research. It is generally recognized that the transcription factor *RUNX3*, which is a key effector of the *TGF-β* signaling pathway, acts on the *TGF-β* receptor, thereby promoting cell proliferation and apoptosis through the *TGF-β* signal transduction pathway (7,10,32-34). This may explain its wide involvement in tumorigenesis (35). However, several other signaling pathways are affected by *RUNX3*. The *Wnt* signaling pathway was confirmed to be associated with *RUNX3* in intestinal tumorigenesis (36) through the formation of a ternary complex with *β-catenin/TCF4* and attenuation of *Wnt* signaling activity, whereas the inactivation of *RUNX3* may promote intestinal adenoma formation (36). In addition, the mitochondria-mediated pathway has been demonstrated to be associated with *RUNX3*, inducing apoptosis in gastric cancer cells (37). In a study on hepatocellular carcinoma (HCC), the researchers reported that *RUNX3* suppressed *Notch* signaling in HCC SMMC7721 cells (38). In the present study, the *TNF* and *FoxO* signaling pathways were demonstrated to be associated with *RUNX3*.

TNF is a member of the *TNF* superfamily of cytokines, which mediates cell processes such as differentiation, inflam-

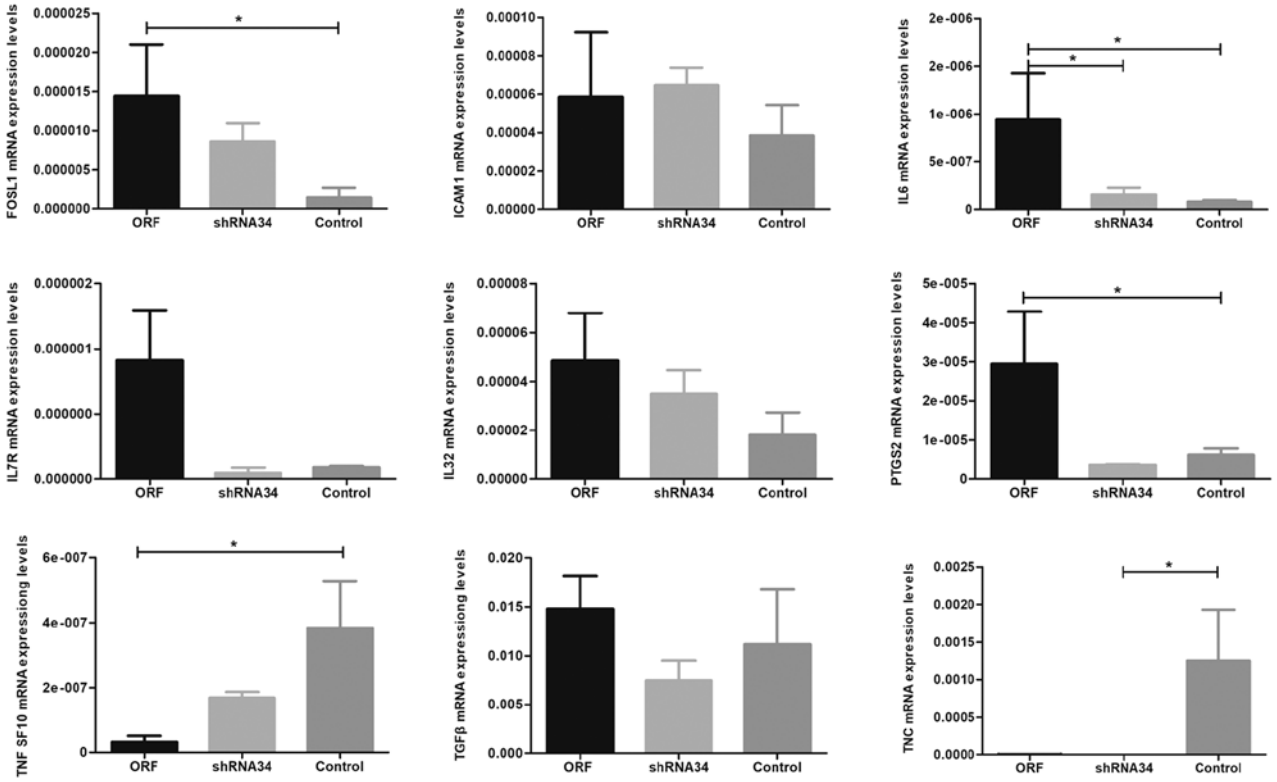

Figure 7. mRNA expression levels of different genes were partly consistent with the results of transcriptome sequencing in cervical cancer cells, which were all confirmed in SiHa, HeLa and C33A cell lines. *P<0.05. ORF, *RUNX3* overexpression cells; *RUNX3*, Runt-related transcription factor 3; shRNA, short hairpin RNA.

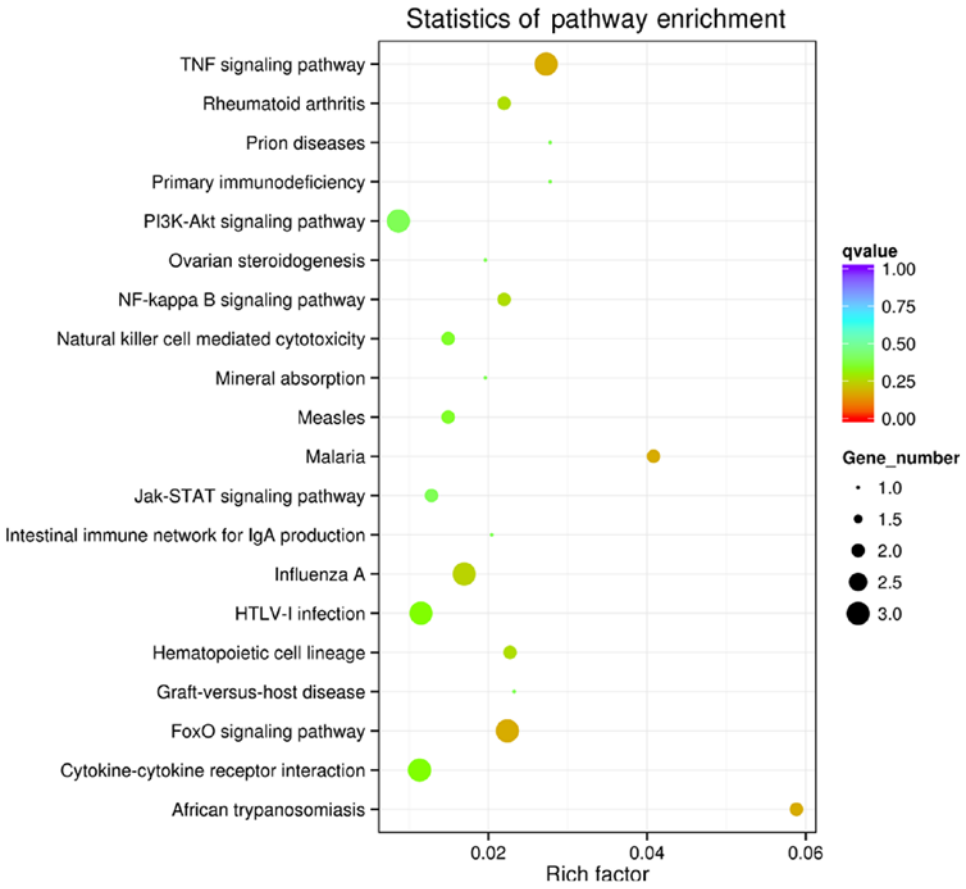

Figure 8. Signaling pathways potentially involved in *RUNX3*-overexpressing cells with Kyoto Encyclopedia of Genes and Genomes enrichment analysis. The size of the point indicates the number of differentially expressed genes in the pathway, and the color of the point corresponds to a different q value range. *RUNX3*, Runt-related transcription factor 3; q value, P-adjusted value.

mation, proliferation and apoptosis (39), and has double the effect in cancer cells. More specifically, it has been reported that *TNF* is associated with cervical cancer (40). In addition, the *TNF-α/TNFR1/NF-κB* pathway is potentially implicated in tongue cancer and lung metastasis (41). The *NF-κB* signaling axis (defined by the interactions of *NF-κB* dimers, *IκB* regulators and *IKK* complexes) is responsive to external stimuli and signal received (42). *FoxO* is a subfamily member of the forkhead transcription factor family. *FoxO* has been revealed as a key determinant of cell fate, and to play an important functional role as a tumor suppressor in different types of cancer (43,44). During apoptosis, *FoxO* is involved in mitochondria-dependent and -independent processes that trigger the expression of death receptor ligands, such as Fas ligand, *TNF* apoptosis ligand, *Bcl XL*, *bNIP3* and *Bim* (43,44). The most important pathway associated with *FoxO* is the *PI3K/AKT* pathway. The *PI3K/AKT* pathway is also dysregulated and activated in a wide variety of cancers, such as breast, thyroid and cervical cancers (43). In addition, the *Ras/MEK/ERK, IKK* and *AMPK* pathways have also been demonstrated to be associated with *FoxO*, and they may play a role in tumorigenesis (43-45). However, the role of *FoxO* in cervical cancer has not been extensively investigated. An association between *FoxO* and *TGF-β* in tumors has also been reported (46,47). In an HCC study, the Thr32 residue of *FoxO3* was proven to be a critical factor for *TGF-β*-induced apoptosis, which was mediated via *Bim* (47). Due to the complexity and uncertainty of the associations between *RUNX3* and signaling pathways, further research is required in order to confirm the association between *RUNX3* and the *TNF/FoxO* pathway in cervical cancer.

Recently, the associations of lncRNAs with *RUNX3* in different cancers were investigated. A previous study identified a potential competing endogenous RNA regulatory network involving *MT1JP* and the regulation of *RUNX3* expression and progression of gastric cancer (48). In a study of human colorectal cancer, *miR-532-5p* mimic was revealed to markedly downregulate the mRNA and protein levels of *RUNX3*, potentially acting as an oncogenic miRNA (49). Finally, the present study demonstrated that *RUNX3* may affect the expression levels of *RP11-54O7.3* and *MALAT1*. According to previous reports, *MALAT1* may participate in tumor formation, such as lung, prostate and ovarian cancer (50-53). It was recently reported that overexpression of *MALAT1* could sponge *miR-429* and regulate cervical cancer pathogenesis *in vivo* and *in vitro* (54), while the associations between *MALAT1* and *RUNX3* remain unclear. However, the role of *RP11-54O7.3* has not yet been fully elucidated, and the association between *RP11-54O7.3* and *RUNX3* remains unknown (55,56). These results indicate that *RUNX3* may affect the expression of *lncRNAs*, which may be associated with cervical cancer *in vitro*. The specific mechanisms of action and role of *RUNX3* in cervical cancer will be further investigated in future studies.

In conclusion, the present study demonstrated that *RUNX3* inhibited proliferation and promoted the apoptosis of cervical cancer cells. In addition, the *TNF* and *FoxO* pathways were demonstrated to be affected by *RUNX3*, and the effects of *MALAT1* and *RP11-54O7.3* are likely mediated by *RUNX3* in cervical cancer. However, further research is required in order to achieve an improved understanding of the molecular complexities and functions of *RUNX3* in cervical cancer.

Acknowledgements

Not applicable.

Funding

The present study was funded by the National Natural Science Foundation of China (grant nos. 81572573 and 81172440), and the New Bud Research Foundation of West China Second University Hospital (grant no. kx091), Sichuan University.

Availability of data and materials

All data generated or analyzed during the present study are included in this published article.

Authors' contributions

XY, ZZ and YS contributed to analysis and manuscript preparation. QG and MX performed the data analyses and wrote the manuscript. BZ, YW, LZ and HL helped perform the analysis with constructive discussions.

Ethics approval and consent to participate

Not applicable.

Patient consent for publication

Not applicable.

Competing interests

The authors declare that they have no competing interests.

References

1. Torre LA, Bray F, Siegel RL, Ferlay J, Lortet-Tieulent J and Jemal A: Global cancer statistics 2012. CA Cancer J Clin 65: 87-108, 2015.
2. Berkhof J, de Bruijne MC, Zielinski GD and Meijer CJ: Natural history and screening model for high-risk human papillomavirus infection, neoplasia and cervical cancer in the Netherlands. Int J Cancer 115: 268-275, 2005.
3. McCredie MR, Sharples KJ, Paul C, Baranyai J, Medley G, Jones RW and Skegg DC: Natural history of cervical neoplasia and risk of invasive cancer in women with cervical intraepithelial neoplasia 3: A retrospective cohort study. Lancet Oncol 9: 425-434, 2008.
4. González-Herrera L, Rodríguez-Morales P, Gonza Lez-Losa Mdel R, Pérez-Mendoza G, Canul-Canché J, Rosado-López I and Cetina TC: MTHFR/p53 polymorphisms as genetic factors for cervical intraepithelial neoplasia and cervical cancer in HPV-infected Mexican women. Int J Biol Markers 29: e142-e149, 2014.
5. Kuglik P, Kasikova K, Smetana J, Vallova V, Lastuvkova A, Moukova L, Cvanova M and Brozova L: Molecular cytogenetic analyses of hTERC (3q26) and MYC (8q24) genes amplifications in correlation with oncogenic human papillomavirus infection in Czech patients with cervical intraepithelial neoplasia and cervical carcinomas. Neoplasma 62: 130-139, 2015.
6. Lund AH and van Lohuizen M: RUNX: A trilogy of cancer genes. Cancer Cell 1: 213-215, 2002.
7. Ito Y and Miyazono K: RUNX transcription factors as key targets of TGF-beta superfamily signaling. Curr Opin Genet Dev 13: 43-47, 2003.

8. Hwang KT, Han W, Bae JY, Hwang SE, Shin HJ, Lee JE, Kim SW, Min HJ and Noh DY: Downregulation of the RUNX3 gene by promoter hypermethylation and hemizygous deletion in breast cancer. J Korean Med Sci 22 (Suppl): S24-S31, 2007.
9. Li QL, Ito K, Sakakura C, Fukamachi H, Inoue K, Chi XZ, Lee KY, Nomura S, Lee CW, Han SB, *et al*: Causal relationship between the loss of RUNX3 expression and gastric cancer. Cell 109: 113-124, 2002.
10. Subramaniam MM, Chan JY, Yeoh KG, Quek T, Ito K and Salto-Tellez M: Molecular pathology of RUNX3 in human carcinogenesis. Biochim Biophys Acta 1796: 315-331, 2009.
11. Xiao WH and Liu WW: Hemizygous deletion and hypermethylation of RUNX3 gene in hepatocellular carcinoma. World J Gastroenterol 10: 376-380, 2004.
12. Li Z, Fan P, Deng M and Zeng C: The roles of RUNX3 in cervical cancer cells *in vitro*. Oncol Lett 15: 8729-8734, 2018.
13. Gao F, Huang C, Lin M, Wang Z, Shen J, Zhang H, Jiang L and Chen Q: Frequent inactivation of RUNX3 by promoter hypermethylation and protein mislocalization in oral squamous cell carcinomas. J Cancer Res Clin Oncol 135: 739-747, 2009.
14. Ito K, Liu Q, Salto-Tellez M, Yano T, Tada K, Ida H, Huang C, Shah N, Inoue M, Rajnakova A, *et al*: RUNX3, a novel tumor suppressor, is frequently inactivated in gastric cancer by protein mislocalization. Cancer Res 65: 7743-7750, 2005.
15. Kim WJ, Kim EJ, Jeong P, Quan C, Kim J, Li QL, Yang JO, Ito Y and Bae SC: RUNX3 inactivation by point mutations and aberrant DNA methylation in bladder tumors. Cancer Res 65: 9347-9354, 2005.
16. Lau QC, Raja E, Salto-Tellez M, Liu Q, Ito K, Inoue M, Putti TC, Loh M, Ko TK, Huang C, *et al*: RUNX3 is frequently inactivated by dual mechanisms of protein mislocalization and promoter hypermethylation in breast cancer. Cancer Res 66: 6512-6520, 2006.
17. Kudo Y, Tsunematsu T and Takata T: Oncogenic role of RUNX3 in head and neck cancer. J Cell Biochem 112: 387-393, 2011.
18. Tsunematsu T, Kudo Y, Iizuka S, Ogawa I, Fujita T, Kurihara H, Abiko Y and Takata T: RUNX3 has an oncogenic role in head and neck cancer. PLoS One 4: e5892, 2009.
19. Lee JH, Pyon JK, Kim DW, Lee SH, Nam HS, Kang SG, Kim CH, Lee YJ, Chun JS and Cho MK: Expression of RUNX3 in skin cancers. Clin Exp Dermatol 36: 769-774, 2011.
20. Häfner N, Steinbach D, Jansen L, Diebolder H, Dürst M and Runnebaum IB: RUNX3 and CAMK2N1 hypermethylation as prognostic marker for epithelial ovarian cancer. INT J Cancer 138: 217-228, 2016.
21. Lotem J, Levanon D, Negreanu V, Bauer O, Hantisteanu S, Dicken J and Groner Y: Runx3 at the interface of immunity, inflammation and cancer. Biochim Biophys Acta 1855: 131-143, 2015.
22. Gao QQ, Zhou B, Yu XZ, Zeng X, Zhang Z, Quan Y, Wang YY, Pu Y, Cheng P, Song YP, *et al*: RUNX3 polymorphisms and the susceptibility to cervical cancer and cervical intraepithelial neoplasia in Western China. Int J Clin Exp Pathol 9: 10617-10626, 2016.
23. Lee JW, Kim DM, Jang JW, Park TG, Song SH, Lee YS, Chi XZ, Park IY, Hyun JW, Ito Y and Bae SC: RUNX3 regulates cell cycle-dependent chromatin dynamics by functioning as a pioneer factor of the restriction-point. Nat Commun 10: 1897, 2019.
24. Livak KJ and Schmittgen TD: Analysis of relative gene expression data using real-time quantitative PCR and the 2(-Delta Delta C(T)) method. Methods 25: 402-408, 2001.
25. Dal Cin P, Fusco A, Belge G, Chiappetta G, Fedele M, Pauwels P, Bullerdiek J and Van den Berghe H: Involvement of the HMGI(Y) gene in a microfollicular adenoma of the thyroid. Genes Chromosomes Cancer 24: 286-289, 1999.
26. Hirata H, Hinoda Y, Shahryari V, Deng G, Nakajima K, Tabatabai ZL, Ishii N and Dahiya R: Long Noncoding RNA MALAT1 promotes aggressive renal cell carcinoma through Ezh2 and interacts with miR-205. Cancer Res 75: 1322-1331, 2015.
27. Quan Y, Zhou B, Wang Y, Duan R, Wang K, Gao Q, Shi S, Song Y, Zhang L and Xi M: Association between IL17 polymorphisms and risk of cervical cancer in Chinese women. Clin Dev Immunol 2012: 258-293, 2012.
28. Walch-Rückheim B, Mavrova R, Henning M, Vicinus B, Kim YJ, Bohle RM, Juhasz-Böss I, Solomayer EF and Smola S: Stromal fibroblasts induce CCL20 through IL6/C/EBPβ to support the recruitment of Th17 cells during cervical cancer progression. Cancer Res 75: 5248-5259, 2015.
29. Zidi S, Sghaier I, Gazouani E, Mezlini A and Yacoubi-Loueslati B: Evaluation of Toll-like receptors 2/3/4/9 gene polymorphisms in cervical cancer evolution. Pathol Oncol Res 22: 323-330, 2016.
30. Zidi S, Stayoussef M, Gazouani E, Mezlini A, Yacoubi-Loueslati B and Almawi WY: Relationship of common vascular endothelial growth factor polymorphisms and haplotypes with the risk of cervical cancer in Tunisians. Cytokine 74: 108-112, 2015.
31. Barghout SH, Zepeda N, Vincent K, Azad AK, Xu Z, Yang C, Steed H, Postovit LM and Fu Y: RUNX3 contributes to carboplatin resistance in epithelial ovarian cancer cells. Gynecol Oncol 138: 647-655, 2015.
32. Yano T, Ito K, Fukamachi H, Chi XZ, Wee HJ, Inoue K, Ida H, Bouillet P, Strasser A, Bae SC and Ito Y: The RUNX3 tumor suppressor upregulates Bim in gastric epithelial cells undergoing transforming growth factor beta-induced apoptosis. Mol Cell Biol 26: 4474-4488, 2006.
33. Yamamura Y, Lee WL, Inoue K, Ida H and Ito Y: RUNX3 cooperates with FoxO3a to induce apoptosis in gastric cancer cells. J Biol Chem 281: 5267-5276, 2006.
34. Chi XZ, Yang JO, Lee KY, Ito K, Sakakura C, Li QL, Kim HR, Cha EJ, Lee YH, Kaneda A, *et al*: RUNX3 suppresses gastric epithelial cell growth by inducing p21(WAF1/Cip1) expression in cooperation with transforming growth factor {beta}-activated SMAD. Mol Cell Biol 25: 8097-8107, 2005.
35. Farooqi AA, Khalid S and Ahmad A: Regulation of cell signaling pathways and miRNAs by resveratrol in different cancers. Int J Mol Sci 19: pii: E652, 2018.
36. Ito K, Lim AC, Salto-Tellez M, Motoda L, Osato M, Chuang LS, Lee CW, Voon DC, Koo JK, Wang H, *et al*: RUNX3 attenuates beta-catenin/T cell factors in intestinal tumorigenesis. Cancer Cell 14: 226-237, 2008.
37. Nagahama Y, Ishimaru M, Osaki M, Inoue T, Maeda A, Nakada C, Moriyama M, Sato K, Oshimura M and Ito H: Apoptotic pathway induced by transduction of RUNX3 in the human gastric carcinoma cell line MKN-1. Cancer Sci 99: 23-30, 2008.
38. Gao J, Chen Y, Wu KC, Liu J, Zhao YQ, Pan YL, Du R, Zheng GR, Xiong YM, Xu HL and Fan DM: RUNX3 directly interacts with intracellular domain of Notch1 and suppresses Notch signaling in hepatocellular carcinoma cells. Exp Cell Res 316: 149-157, 2010.
39. Holdbrooks AT, Britain CM and Bellis SL: ST6Gal-I sialyltransferase promotes tumor necrosis factor (TNF)-mediated cancer cell survival via sialylation of the TNF receptor 1 (TNFR1) death receptor. J Biol Chem 293: 1610-1622, 2018.
40. Zidi S, Stayoussef M, Zouidi F, Benali S, Gazouani E, Mezlini A and Yacoubi-Loueslati B: Tumor necrosis factor alpha (-238/-308) and TNFRII-VNTR (-322) polymorphisms as genetic biomarkers of susceptibility to develop cervical cancer among tunisians. Pathol Oncol Res 21: 339-345, 2015.
41. Tanaka T, Imamura T, Yoneda M, Irie A, Ogi H, Nagata M, Yoshida R, Fukuma D, Kawahara K, Shinohara M and Nakayama H: Enhancement of active MMP release and invasive activity of lymph node metastatic tongue cancer cells by elevated signaling via the TNF-α-TNFR1-NF-κB pathway and a possible involvement of angiopoietin-like 4 in lung metastasis. Int J Oncol 49: 1377-1384, 2016.
42. Mitchell S, Vargas J and Hoffmann A: Signaling via the NFκB system. Wiley Interdiscip Rev Syst Biol Med 8: 227-241, 2016.
43. Farhan M, Wang H, Gaur U, Little PJ, Xu J and Zheng W: foxo signaling pathways as therapeutic targets in cancer. Int J Biol Sci 13: 815-827, 2017.
44. Coomans de Brachène A and Demoulin JB: FOXO transcription factors in cancer development and therapy. Cell Mol Life Sci 73: 1159-1172, 2016.
45. Link W and Fernandez-Marcos PJ: FOXO transcription factors at the interface of metabolism and cancer. Int J Cancer 141: 2379-2391, 2017.
46. Yadav H, Devalaraja S, Chung ST and Rane SG: TGF-β1/Smad3 pathway targets PP2A-AMPK-FoxO1 signaling to regulate hepatic gluconeogenesis. J Biol Chem 292: 3420-3432, 2017.
47. Zhao X, Liu Y, Du L, He L, Ni B, Hu J, Zhu D and Chen Q: Threonine 32 (Thr32) of FoxO3 is critical for TGF-β-induced apoptosis via Bim in hepatocarcinoma cells. Protein Cell 6: 127-138, 2015.
48. Xu Y, Zhang G, Zou C, Zhang H, Gong Z, Wang W, Ma G, Jiang P and Zhang W: LncRNA MT1JP suppresses gastric cancer cell proliferation and migration through MT1JP/MiR-214-3p/RUNX3 axis. Cell Physiol Biochem 46: 2445-2459, 2018.
49. Zhang J, Zhou W, Liu Y, Liu T, Li C and Wang L: Oncogenic role of microRNA-532-5p in human colorectal cancer via targeting of the 5'UTR of RUNX3. Oncol Lett 15: 7215-7220, 2018.
50. Xue D, Lu H, Xu HY, Zhou CX and He XZ: Long noncoding RNA MALAT1 enhances the docetaxel resistance of prostate cancer cells via miR-145-5p-mediated regulation of AKAP12. J Cell Mol Med 22: 3223-3237, 2018.

51. Bai L, Wang A, Zhang Y, Xu X and Zhang X: Knockdown of MALAT1 enhances chemosensitivity of ovarian cancer cells to cisplatin through inhibiting the Notch1 signaling pathway. Exp Cell Res 366: 161-171, 2018.
52. Fang Z, Chen W, Yuan Z, Liu X and Jiang H: LncRNA-MALAT1 contributes to the cisplatin-resistance of lung cancer by upregulating MRP1 and MDR1 via STAT3 activation. Biomed Pharmacother 101: 536-542, 2018.
53. Xiping Z, Bo C, Shifeng Y, Feijiang Y, Hongjian Y, Qihui C and Binbin T: Roles of MALAT1 in development and migration of triple negative and Her-2 positive breast cancer. Oncotarget 9: 2255-2267, 2017.
54. Shen F, Zheng H, Zhou L, Li W and Xu X: Overexpression of MALAT1 contributes to cervical cancer progression by acting as a sponge of miR-429. J Cell Physiol 234: 11219-11226, 2019.
55. Li J, Wang W, Xia P, Wan L, Zhang L, Yu L, Wang L, Chen X, Xiao Y and Xu C: Identification of a five-lncRNA signature for predicting the risk of tumor recurrence in patients with breast cancer. Int J cancer 143: 2150-2160, 2018.
56. Jiang W, Zhan H, Jiao Y, Li S and Gao W: A novel lncRNA-miRNA-mRNA network analysis identified the hub lncRNA RP11-159F24.1 in the pathogenesis of papillary thyroid cancer. Cancer Med 7: 6290-6298, 2018.